RCS CrystEngComm

Supporting Information

A new Insight into the Effect of Mass Transfer on the Synthesis of Silver and Gold Nanoparticles

Maximilian O. Besenhard,[a] Razwan Baber,[a] Alec P. LaGrow,[b] Luca Mazzei,[a] Nguyen T.K. Thanh [b,c,]* and Asterios Gavriilidis [a,]*

---

[a] *Department of Chemical Engineering, University College London, Torrington Place, London, WC1E 7JE, UK*

[b] *UCL Healthcare Biomagnetic and Nanomaterials Laboratories, 21 Albemarle Street, London W1S 4BS, UK*

[c] *Biophysics Group, Department of Physics and Astronomy, University College London, Gower Street, London WC1E 6BT, UK*

* *Corresponding authors.*

Email: ntk.thanh@ucl.ac.uk and a.gavriilidis@ucl.ac.uk

1 Triiodide extinction coefficient determination

A known concentration of iodine was prepared by mixing a stoichiometric balance of solutions containing iodide and iodate ions. To this mixture, an excess of sulfuric acid was added to convert all the iodide and iodate to iodine according to the following reaction:

$$IO_3^- + 5I^- + 6H^+ \rightarrow 3I_2 + 3H_2O$$

Therefore, a 14.2 mM H_2SO_4 solution was added to a mixture of 2.26 mM KI solution and 0.452 mM KIO_3 solution of equal volumes (*i.e.,* the volume of acid is equal to that of the iodide/iodate mixture). This resulted in a concentration after mixing of 7.1 mM H_2SO_4, 1.13 mM KI and 0.226 mM of KIO_3. By combining these reagents in the quantities above, the following iodine concentrations were obtained:

$$5[IO_3^-] = [I^-] = \frac{5}{3}[I_2] = 1.13\,mM$$

$$[I_2] = 0.68\,mM$$

Using this solution (100%) and dilutions to 80%, 60%, 40% and 20% absorbance values at 460 nm (wavelength at which iodine absorbs light significantly) were obtained as shown in Figure S1. An extinction coefficient for iodine of 626 l/(mol·cm) was determined from the increase in absorbance with concentration. A value of 758 l/(mol·cm) has been reported for iodine at 460 nm.[1]

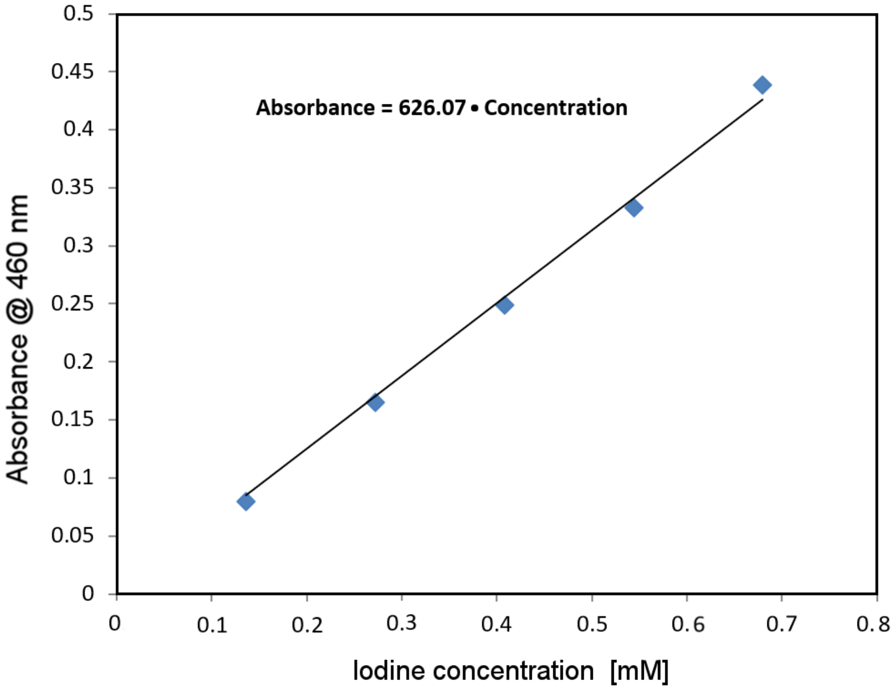

Figure S1: Calibration curve for iodine, absorbance vs. concentration, with the linear fit used to obtain the extinction coefficient of iodine.

Solutions with the relevant triiodide concentration were prepared to determine the triiodide extinction coefficient following a similar procedure, *i.e.,* the saturation method. Therefore, known amounts of iodine were mixed with an excess of iodide. The large excess of iodide ions (saturation) drives the equilibrium largely in favour of the triiodide ion ($I^- + I_2 \leftrightarrow I_3^-$; reaction 3 in the main article). Hence, the known iodine concentration determines the solution triiodide concentration.

Thus, 1 ml of a 0.321 M KI solution was added per 1 ml iodine solution of a significantly lower iodine concentration ($[I_2] << 0.321$ M; iodine concentration determined *via* UV-Vis spectroscopy, see Figure S1). This solution was then diluted accordingly, and the absorbance was measured at 353 nm to obtain the calibration curve and extinction coefficient for triiodide, see Figure S2. From this dilution series a triiodide extinction coefficient of 23,209 l/(mol·cm) was found.

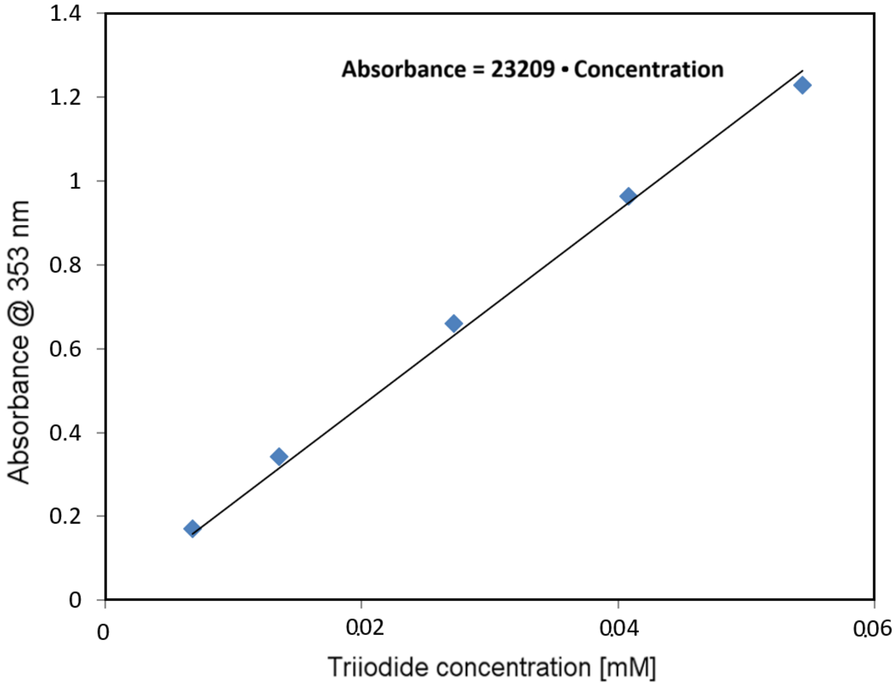

Figure S2: Calibration curve for triiodide, absorbance vs. concentration, with the linear fit used to obtain the extinction coefficient of triiodide.

2 Interaction by exchange with the mean mixing model

The interaction by exchange with the mean (IEM) mixing model can be expressed as follows:[2]

$$\frac{dC_{k,1}(t)}{dt} = \frac{\langle C_k(t)\rangle - C_{k,1}(t)}{t_\mu} + R_{k,1} \tag{1}$$

$$\frac{dC_{k,2}(t)}{dt} = \frac{\langle C_k(t)\rangle - C_{k,2(t)}}{t_\mu} + R_{k,2} \tag{2}$$

$$\langle C_k(t)\rangle = \alpha C_{k,1}(t) + (1-\alpha)C_{k,2}(t) \tag{3}$$

where C_k is concentration of species k, $\langle C_k\rangle$ is the average concentration of species k across acid (sub index 1) and buffer solution (sub index 2), R_k is the reaction rate of species k (obtained from Fournier *et al.* [3]), t_μ is the mixing time and α is the volume fraction of the added acid solution. These equations form the differential mass balance equations that need to be solved to obtain the concentration of triiodide (or segregation index) for a given mixing time according to the model. The segregation index X_s is defined as:

$$X_s = Y / Y_{ST} \tag{4}$$

where Y is the ratio of acid mole number consumed by reaction 2 divided by the total acid mole number injected:

$$Y = \frac{2\cdot \mathrm{V}_{buffer}\cdot\left[C_{I_2,2}\,(t=final) + C_{I_3^-,2}(t=final)\right]}{\mathrm{V}_{acid}\cdot C_{H^+,2}(t=0)} \tag{5}$$

and Y_{ST} is the value of Y when the mixing process is infinitely slow, *i.e.* reactions **(1)** and **(2)** (referring to the main article) become quasi-instantaneous compared to the mixing time (=perfect segregation):

$$Y_{ST} = \frac{6\cdot C_{IO_3{}^-,2}\,(t=0)}{6\cdot C_{IO_3{}^-,2}\,(t=0) + C_{H_2BO_3{}^-,2}\,(t=0)} \tag{6}$$

Further information about the derivation of the segregation index and the system of reaction equations to be solved by the IEM mixing model can be found in the works of Guichardon, Falk, and Commenge. [4, 5] X_s can be determined experimentally by calculating the iodine concentrations *via* the initial ($t = 0$) iodide concentration and the triiodide concentration after mixing ($t = final$; determined using UV-Vis spectroscopy) as described in the previously cited works.

A curve of mixing time vs. triiodide concentration or segregation index can be obtained by setting the initial concentration of the reagents and then solving the mathematical model (here the IEM mixing model) for a range of mixing times. The curve of segregation index vs. mixing time is shown in Figure S3.

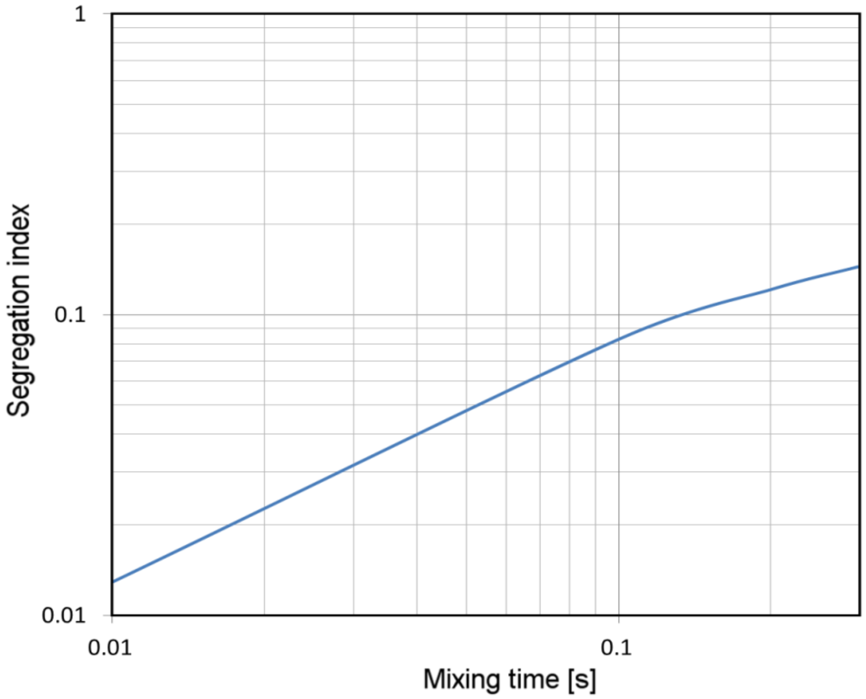

Figure S3: Segregation index vs. mixing time estimated using the IEM model for the Villermaux-Dushman reaction scheme. Concentrations of buffer solution were KI: 0.0117 M, KIO_3; 0.0023 M, NaOH; 0.0909 M, H_3BO_3; 0.1818 M. Concentration of H_2SO_4 was: 0.07 M.

3 Silver nanoparticle characterisation by UV-Vis

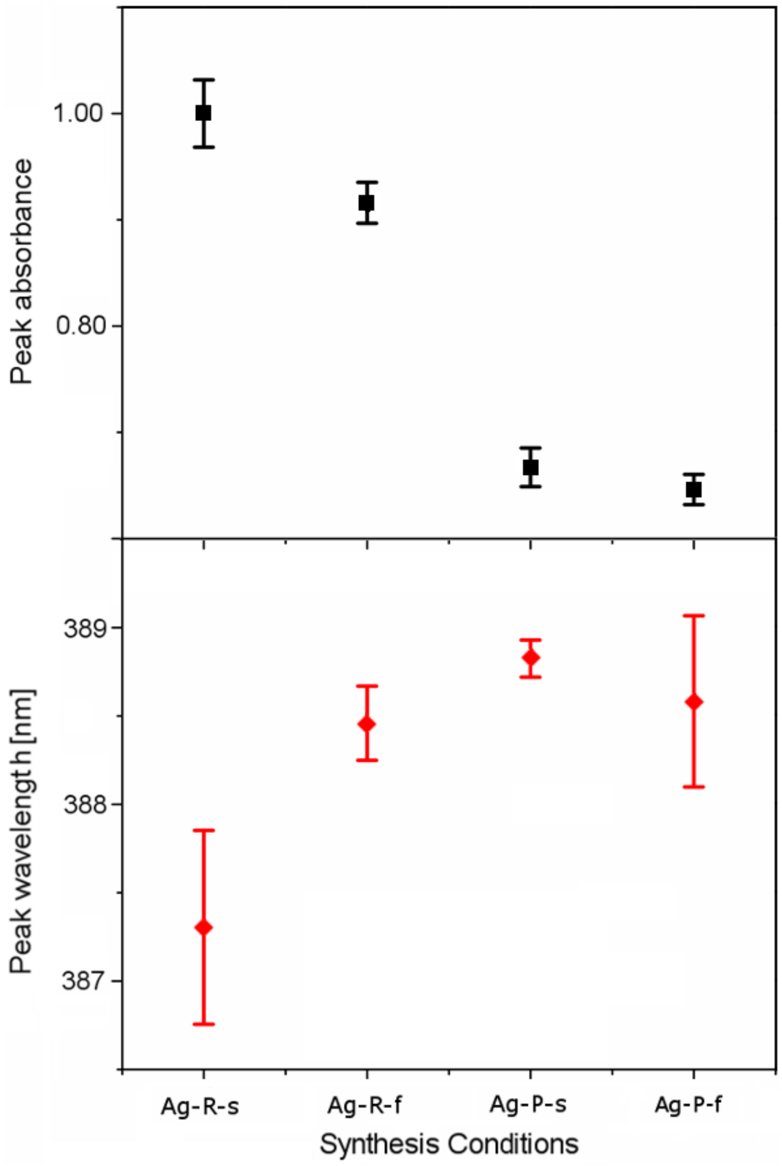

Figure S4: Average peak absorbance and average peak wavelength obtained using UV-Vis spectroscopy of silver NPs synthesized in batch vessel under the synthesis conditions Ag-R-s, Ag-R-f, Ag-P-s, and Ag-P-f. The details of these conditions are listed in Table 1. Note that Ag-P-s and Ag-P-f had lower $AgNO_3$ concentrations than Ag-R-s and Ag-R-f, which explains their lower absorbance values. Error bars represent standard deviations of the absorbance and wavelength of experiments performed in triplicate (*i.e.* UV-Vis spectra recorded after three silver NP syntheses with the same protocol).

4 Gold nanoparticle characterisation by UV-Vis

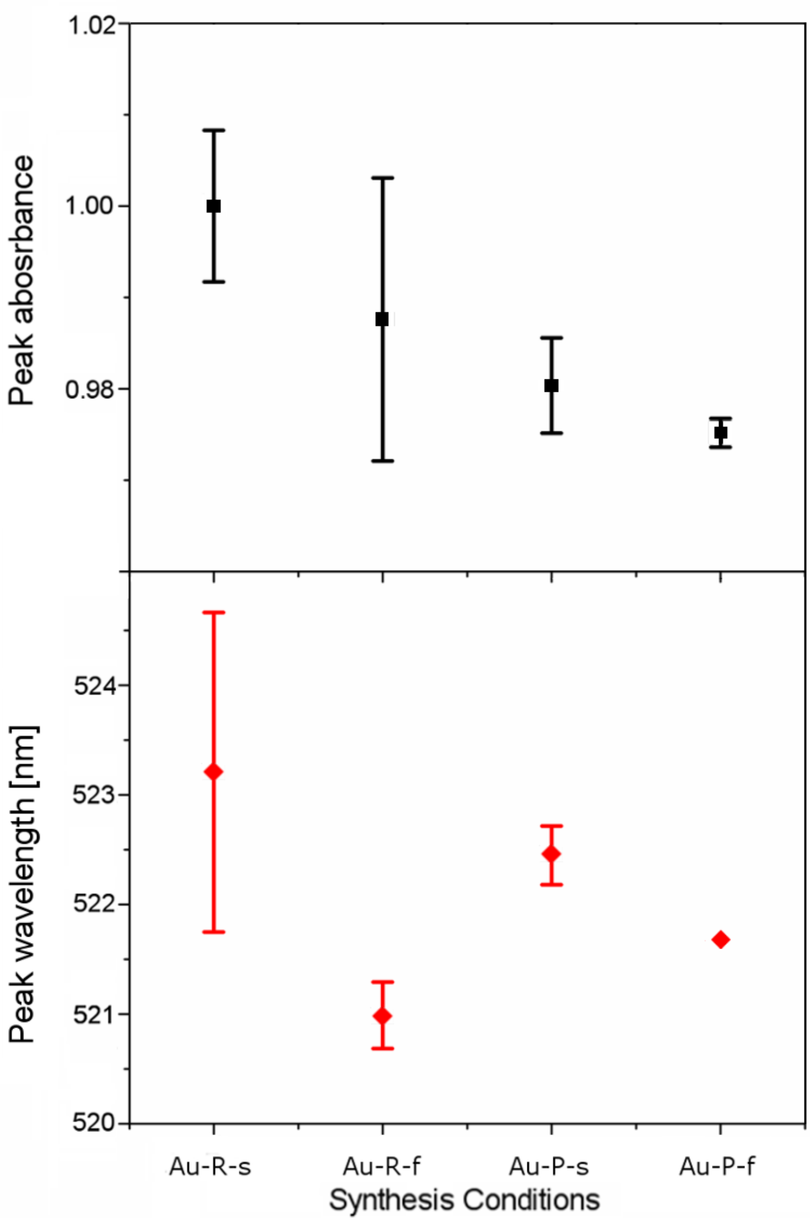

Figure S5: Average peak absorbance and average peak wavelength obtained using UV-Vis spectroscopy of gold NPs synthesized in batch vessel under the synthesis conditions Au-R-s, Au-R-f, Au-P-s, and Au-P-f. The details of these conditions are listed in Table 2. Error bars represent standard deviations of the absorbance and wavelength of experiments performed in triplicate (*i.e.* UV-Vis spectra recorded after three silver NP syntheses with the same protocol).

5 Online UV-Vis studies during silver nanoparticle synthesis

Online UV-Vis spectroscopy was used to monitor changes in the UV-Vis spectrum of the Ag nanoparticle solution during synthesis (Ag-R-s & Ag-P-s) using the set-up shown in Figure S6. The solution was recycled *via* a peristaltic pump pumping the solution through a flow cell of the UV-Vis spectrometer. The inner diameter of tubing was small (2 mm for the peristaltic pump, 1 mm in the flow cell, 0.5 mm otherwise) to reduce the volume of recycled solution. Approximately 0.5 ml of solution, *i.e.* ~ 2.5 % of the volume, was in the recirculation tubing. The recycle time, *i.e.* time it took from source to drain, was in the order of a ~3 s.

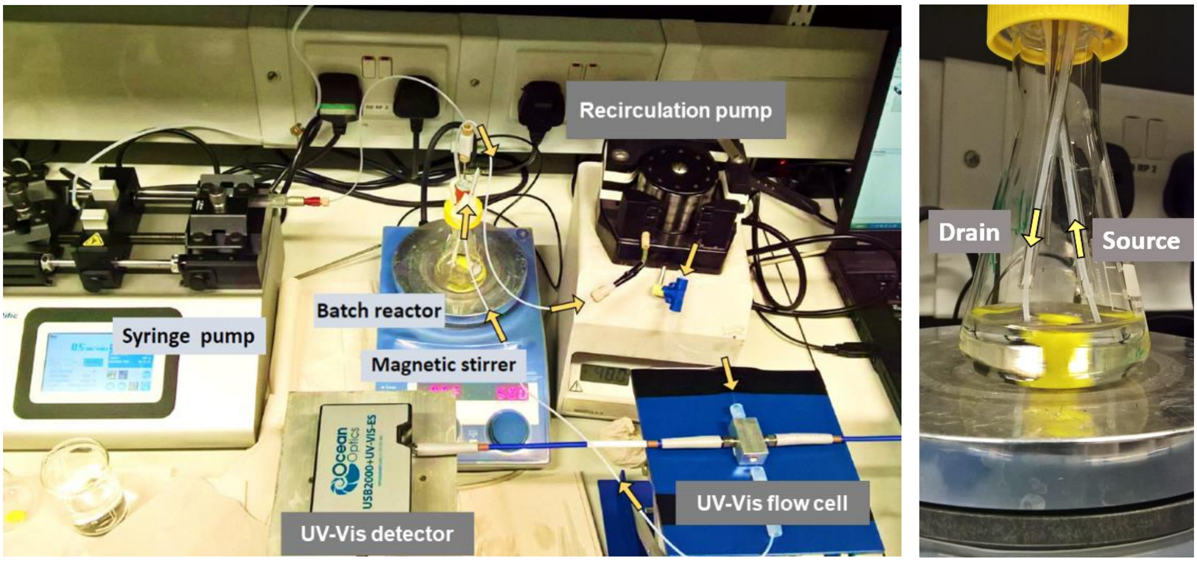

Figure S6: Set-up for online UV-Vis measurements. (*left*) Arrangement of pumps and spectrometer to continuously pump solution from the batch reactor through the UV-Vis flow cell. Parts relevant for the UV-Vis measurements are labelled in white. The yellow arrows indicate the flow direction of the silver nanoparticle solution. (*right*) Batch reactor used, allowing for continuous withdrawal and backflow into the beaker.

The online UV-Vis studies were performed either during the Ag-R-s and Ag-P-s syntheses (see Table 1) or during stepwise addition of either the reducing agent (adapted Ag-R-s synthesis) or the precursor solution (adapted Ag-P-s synthesis). UV-Vis spectra recorded during the Ag-R-s and Ag-P-s syntheses are shown in Figure 3. Stepwise addition refers to the addition of 0.6 ml reducing agent or precursor solution in six steps, *i.e.* every minute 0.1 ml fed at 0.5 ml/min (12 s of feeding every minute till the total volume of 0.6 ml was fed). The UV-Vis spectra recorded continuously during this stepwise addition are shown in Figure S7 and Figure S8.

It is apparent from Figure S7 (adapted Ag-R-s synthesis) that there is no significant change in the UV-Vis spectra after the addition of the first 0.1 ml of the reducing agent solution. This indicates that the solid phase formation is complete after adding less than 20% of the final amount of reducing agent solution. Conclusions about the kinetics in the first seconds after reducing agent addition are hard to draw owing to the mentioned recycle time of the set-up. In contrast, Figure S8 (adapted Ag-P-s synthesis) shows that the absorption during the synthesis Ag-P-s increases with the quantity of added precursor solution.

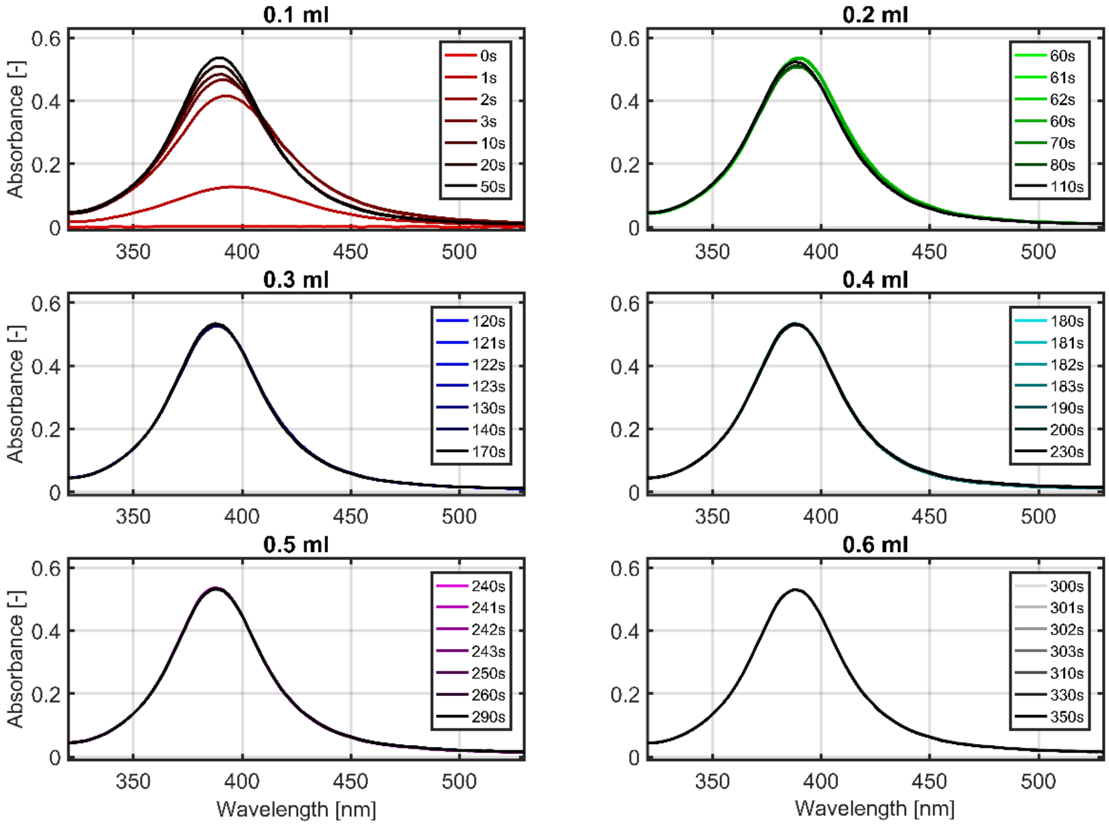

Figure S7: UV-Vis spectra recorded during adapted Ag-R-s synthesis, *i.e.*, performed *via* stepwise (instead of continuous) addition of reducing agent solution (6 steps, every minute new addition of 0.1 ml at 0.5 ml/min).

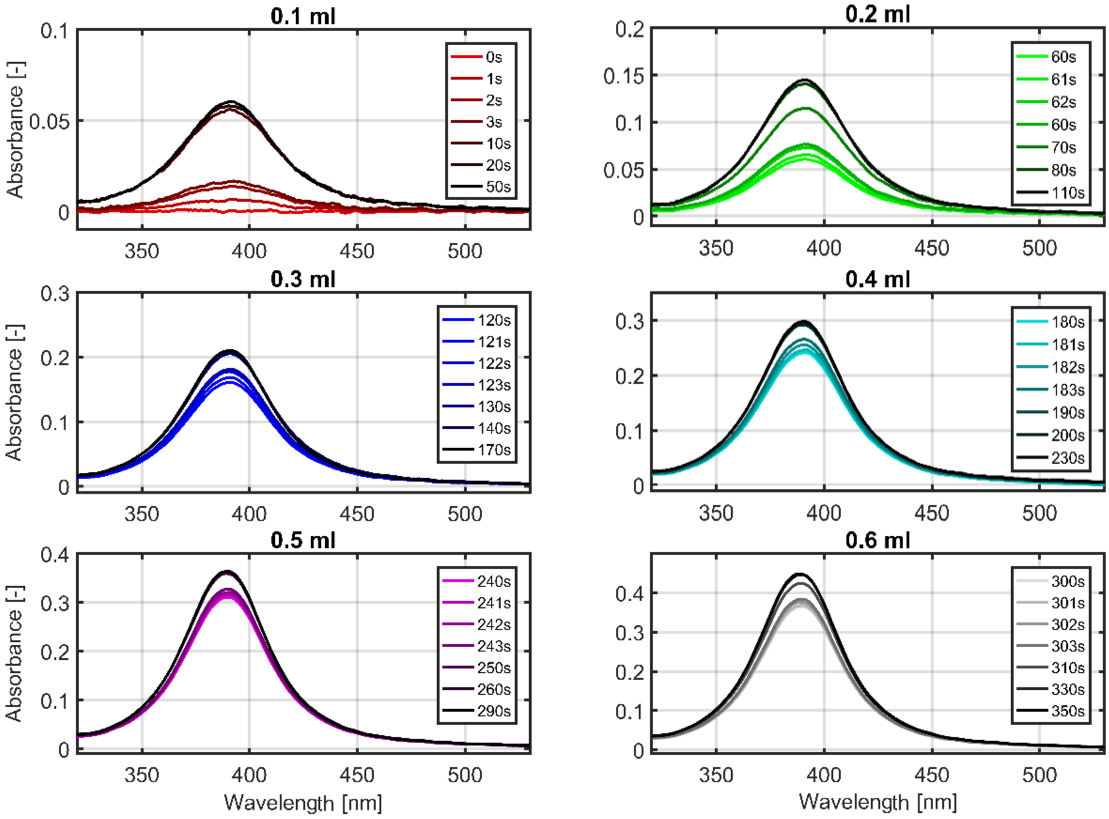

Figure S8: UV-Vis spectra recorded during adapted Ag-P-s synthesis, *i.e.,* performed *via* stepwise (instead of continuous) addition of precursor solution (6 steps, every minute new addition of 0.1 ml at 0.5 ml/min).

6 Silver nanoparticle characterisation by DLS

Figure S9 shows the DLS analysis (zeta potential and size) of the syntheses Ag-P-s and Ag-P-f. The presence of larger particles (> 100 nm) mentioned in the main article explains why the size and zeta potential values for Ag-P-s and Ag-P-f shown in Figure S9 cannot be assigned to the silver NPs. Since larger particles scatter more (the intensity of scattered light is proportional to the sixth power of the particle size) the measured zeta potential values in Figure S9a must be assigned to this larger aggregates (maybe with the exception of the 5 min Ag-P-s sample).

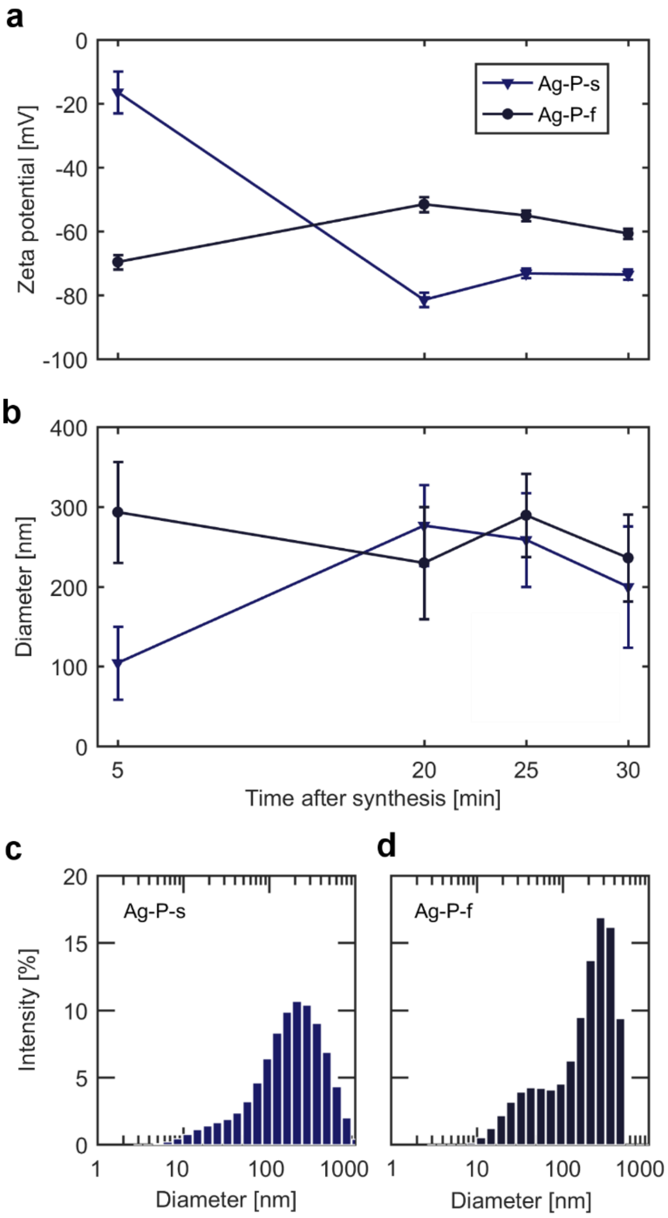

Figure S9: Silver NP characteristics obtained by DLS after the Ag-P-s and Ag-P-f syntheses. Temporal behaviour of (**a**) the zeta potential and (**b**) the intensity weighted diameter after finishing the addition of reducing agent or precursor solution. The error bars show the standard deviation of the five measurements performed for each sample. Size distributions as obtained via DLS for samples taken after 30 min; (**c**) Ag-P-s and (**d**) Ag-P-f.

References

1. Burns, W. G.; Matsuda, M.; Sims, H. E. *Journal of the Chemical Society, Faraday Transactions* **1990,** 86, (9), 1443-1447.
2. Villermaux, J.; Falk, L. *Chem Eng Sci* **1994,** 49, 5127-5140.
3. Fournier, M.-C.; Falk, L.; Villermaux, J. *Chemical Engineering Science* **1996,** 51, 5187-5192.
4. Guichardon, P.; Falk, L. *Chemical Engineering Science* **2000,** 55, 4233-4243.
5. Commenge, J.-M.; Falk, L. *Chemical Engineering and Processing: Process Intensification* **2011,** 50, 979-990.